Experimental study on the impact of reactant gas pressure in the conversion of coal char to combustible gas products in the context of Underground Coal Gasification

Eleni Konstantinou[a,*]

konstantinoue@cardiff.ac.uk

elkostadinou@yahoo.gr

Richard Marsh[b]

[a]Geoenvironmental Research Centre, Cardiff School of Engineering, Cardiff University, UK

[b]Institute of Energy, Cardiff School of Engineering, Cardiff University, UK

*Corresponding author. Tel.: +44 (0)7876725065.

Abstract

This paper describes an experimental investigation to determine the impact of pressurised reactor conditions within the reduction zone of a gasification process employing a semi-batch reactor with a bituminous coal. The conditions examined with this bespoke pressurised rig were designed to be representative of an Underground Coal Gasification (UCG) process, at pressures up to 3.0 MPa and temperatures up to 900 °C; coal samples were approximately 36 g per test. Current published literature suggests that one of the key controlling factors in the conversion and yield within such processes is the behaviour of the pyrolysed coal (char) in the reduction zone of the UCG cavity. This was achieved by using carbon dioxide and steam as the primary reductants with char derived from bituminous coal at a variety of pressure and temperature levels, plus at a range of relative H_2O/CO_2 proportions. The composition of the resulting product gas was measured and subsequently used to calculate cold gas efficiency and carbon conversion (during 90 min at steady state). A shrinking core model was then employed to determine the activation energy and pre-exponential factor under these conditions. The results were then used to extrapolate the contribution of the reduction zone in published research including UCG field trials where discrete analysis of the zones within the gasification cavity was not possible. It was shown that pressure increases the reduction–gasification process of the char in terms of carbon conversion, cold gas efficiency and heating value of the product gas. Under the conditions evaluated herein, optimum gasification conditions for the bituminous coal were determined as 1.65 MPa at H_2O/CO_2 ratio of 2:1 by mass at 900 °C which produced a syngas with a composition of 17.4% CO, 3% CH_4, 42.1% H_2 and LHV of 7.8 MJ/Nm^3.

Keywords: UCG; Underground Coal Gasification; High pressure; Carbon dioxide–steam gasification; Coal char

1 Introduction

Underground Coal Gasification (UCG) is the process by which unmineable coal resources are converted in situ into a combustible gas. Pressurised oxidants such as steam and air or oxygen are injected into the coal seam in order to react with coal and form a product gas. The main gases produced are H_2, CO, CH_4 and CO_2, in proportions depending on temperature, pressure and the composition of the reactant gases injected [1–3]. Although it can be challenging to accurately measure or reproduce these conditions in a reliable fashion, it is generally believed that at high enough temperatures, free oxygen reacts completely with the solid carbon within a relatively short distance from the injection point. The heat evolved acts to pyrolyse the adjacent coal and the char formed then reacts with carbon dioxide, steam or other gases formed by combustion and pyrolysis [4–6]. The key substance, and hence driver of the net gasification process under these conditions is therefore CO_2 which is produced during the oxidation zone [5,7,8]. At the reduction zone CO_2 and steam, which is either introduced deliberately into the cavity or is flowing into the cavity from the oxidation of the surrounding strata, reacts with char and produces around 60% of the total gas product (by volume) during the UCG process. The remaining 40% is produced during the devolatilisation phase, although this is highly dependent on reactor condition, the type of coal and the gaseous reactants [4].

Fig. 1 illustrates the three reaction zones of a reacting channel during a UCG process, which are the oxidation, reduction and pyrolysis zones. During the oxidation zone, as the coal is consumed more coal falls into the growing void, which creates a high coal surface area available for reaction and permits contact between the hot gases and the coal [5,7]. This area is the final reduction zone which converts excess CO_2 to CO and is responsible for the uniform quality of the product gas. Measurement of the upstream gas composition in the oxidation zone has shown comparatively low heating values which demonstrate that the reactions in the oxidation zone do not have such a significant effect on the product gas composition [8,9]. Finally the pyrolysis zone is where the devolatilisation of the coal takes place, forming char that contains active sites for subsequent gas–solid reactions.

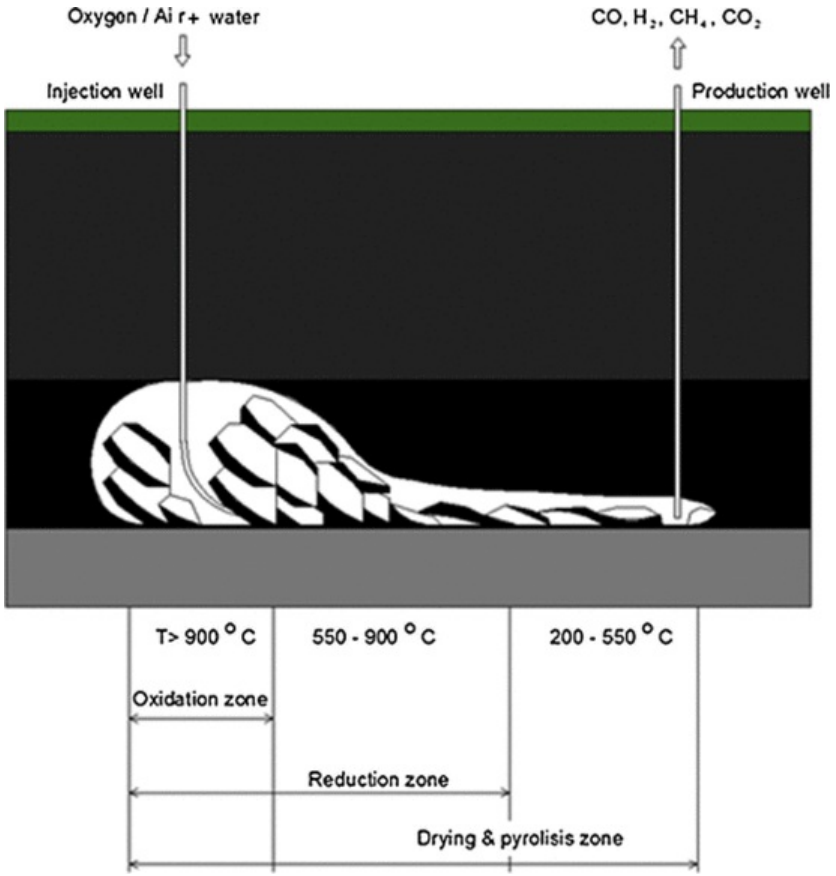

Fig. 1 The three reaction zones of an underground coal gasification channel.

In this work some of the key parameters controlling in situ UCG via a laboratory scale reactor are studied; hence the aim of this research is to demonstrate the effect of the reduction zone reactions at a variety of temperatures and compare this impact to previously published work on UCG field trials. Gasification conditions were established so as to simulate the reduction zone of the UCG process, as this has been identified as a primary controlling factor in the overall mass and energy balance in UCG processes. The effect of the main operating parameters, which included pressure, temperature, flow rates and composition of gaseous reactants were studied. The outputs from the experiments included carbon conversion, cold gas efficiency (CGE) and lower heating value (LHV) of the product gas, which can be used to quantify the effective 'efficiency' of the reduction zone of a UCG process and the suitability of the coal seam for a UCG project. In comparable work by other authors, Chapell (1998) theoretically expressed the efficiency of the gasification process by defining the autothermal chemical equilibrium (ACE) which is a condition at which the heating value of the product gas and the conversion efficiency of the gasified coal (chemical energy of product gas/chemical energy of gasified coal) is a maximum [10]. ACE is identical to CGE within the context of the research undertaken in this paper.

2 Experimental

2.1 Experimental apparatus

Experiments were conducted with a bespoke high pressure, high temperature tubular rig which is shown in Fig. 2 and as a schematic in Fig. 3, and operated at pressures up to 5.0 MPa and 900 °C. This rig consisted of a pressure vessel reactor (10), a carbolite furnace (9), a tar trap (12), a water cooled condenser (13), supplementary gas lines (1) and metering water pump (2). The pressure within the system was governed by a manually operated pressure regulator at the exit of the gas path (14), manually operated pressure regulators on the gas cylinders, a series of computer operated PID mass flow controllers (4), and safety pressure relief valves (7). Pressure levels within the system were monitored with pressure gauges (8), one before and one after the pressure vessel. Non-return valves in incoming gas lines were used to prevent reverse flow in the system (5). The exhaust gas flowrate was measured with a Bronkhorst Coriolis digital mass flow meter (15) before being subjected to on-line quantitative analysis

with analytical equipment (16) described later. The coal samples were held on a quartz boat which was placed in the reactor.

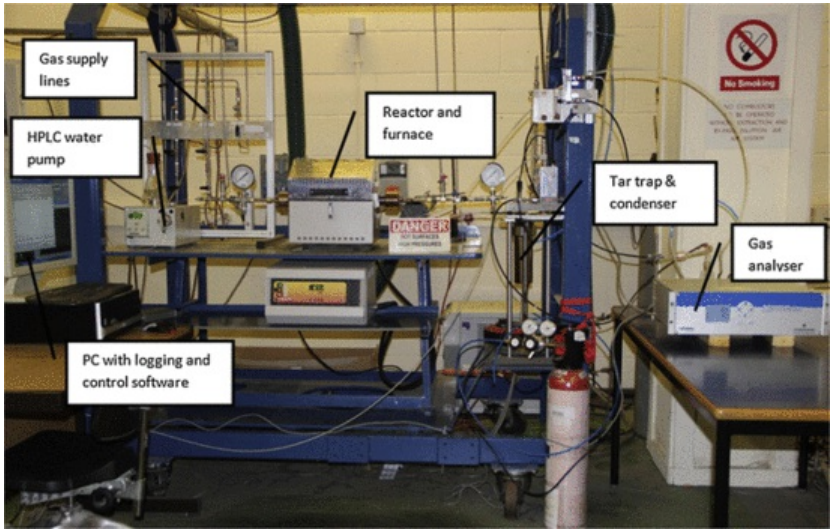

Fig. 2 Image of the bespoke high pressure high temperature rig and associated control and analysis hardware.

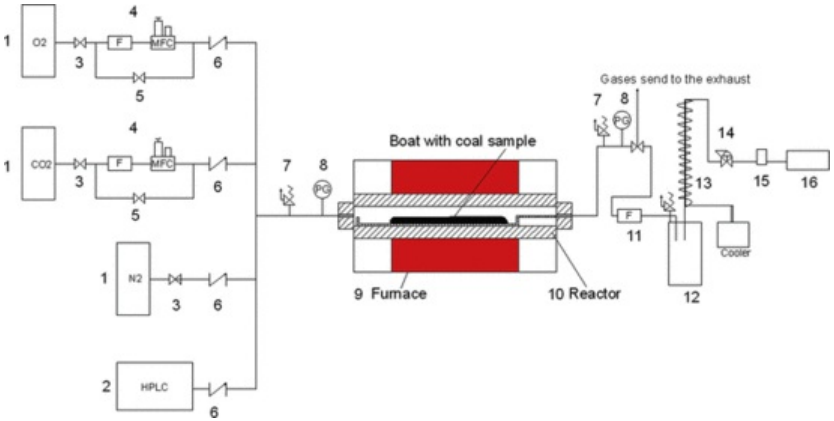

Fig. 3 Schematic of the bespoke high pressure high temperature rig showing the gas supply system (lines of O_2, CO_2, N_2 and steam with mass flow controllers, filters and non-return valves), the reacting system (reactor and furnace with pressure gauges and pressure relief valves before and after the reactor) and the gas analysis system (tar trap, water cooled condenser, cooler, mass flow meter and gas analyser).

2.2 Char preparation

Samples from a bituminous coal were used in this study. Properties of the test coal are described in Table 1. Cylindrical coal samples were extracted from parent fragments with a diamond core drill at 19 mm diameter ~~x~~ x 40 mm length test specimens (with a resulting mass of around 36 g per sample) as shown in Fig. 4. The coal samples were placed on a quartz boat which was introduced into the reactor under a flow of nitrogen. Char was first prepared in the rig in the N_2 environment with a slow heating rate since during the UCG process, the heating rate of the coal seam during pyrolysis is described as slow [8,11]. The temperature of the furnace was increased to the required set point temperature at a rate of 10 °C/min and maintained at that temperature for 30 min until the volatile matter within the coal was released.

Table 1 Proximate, ultimate analysis and LHV of the coal and the prepared char on an 'as received' basis.

Parameters	Units	Bituminous coal	Bituminous coal char
Moisture	%	0.6	0.1
Ash	%	3.3	10.1
Volatile matter	%	13.0	5.4
Fixed carbon	%	83.2	84.4
LHV	MJ/kg	32	31.5
Carbon C	%	88.3	99
Sulphur S	%	0.6	0.9

Fig. 4 Image of the cylindrical coal samples.

2.3 Char gasification

After pyrolysis, the N_2 flow was stopped and reactant gases comprising CO_2 and steam were introduced into the reactor at a variety of ratios, at pressures from 0.1 to 3.0 MPa and temperatures from 600 °C to 900 °C, depending on the conditions under scrutiny. The chemical species of CO, CH_4, H_2 and CO_2 were analysed by an on-line continuous monitoring Emerson X-Stream Enhanced Process Gas Analyser.

2.4 Effect of operation variables

Table 2 shows some of the commonly accepted key chemical reactions that comprise the gasification process between carbon based reactants, including solid carbon and CH_4, with principal oxidants including O_2, CO_2 and H_2O. Although it is extremely challenging to isolate the contribution of these reactions directly, the use of a laboratory rig can highlight some of the resulting concentrations of product gases under prescribed reactor conditions.

Table 2 Principal overall reactions participating in the coal gasification process.

Reaction		Reaction enthalpy	
Oxidation (combustion)	$C + O_2 = CO_2$	$-393\ kJ/mol^{-1}$	(R1)
Partial oxidation	$C + 1/2O_2 = CO$	$-111\ kJ/mol^{-1}$	(R2)
Boudouard	$C + CO_2 = 2CO$	$+172\ kJ/mol^{-1}$	(R3)
Steam–carbon	$C + H_2O = H_2 + CO$	$+131\ kJ/mol^{-1}$	(R4)
Hydrogasification	$C + 2H_2 = CH_4$	$-75\ kJ/mol^{-1}$	(R5)
Water–gas-shift	$CO + H_2O = H_2 + CO_2$	$-41\ kJ/mol^{-1}$	(R6)

Methanation	$CO + 3H_2 = CH_4 + H_2O$	$-206\ kJ/mol^{-1}$	(R7)

Reactions R1 and R2 take place during the oxidation zone where char reacts with O_2 and produces mainly CO_2 and CO plus heat is released. The main reduction reactions which take place are (net) endothermic and hence need heat in order to proceed. These are the gas–solid reactions R3 and R4 in Table 2. Additionally to this, secondary reactions take place which are the homogeneous reactions R6–R7 in Table 2.

The effect of the key operating parameters, such as temperature, flow rates of oxidants and pressure on the product gas composition is presented in this paper. Furthermore other important parameters are determined such as carbon conversion (*X*), CGE and LHV of the product gas, parameters which define the gasification effectiveness in the process. This research is primarily concerned with measuring the processes occurring in the reduction zone of the UGC process. CO_2 was introduced as an oxidant to examine its effect on the solid char material; hence it was not possible to determine the amount of the CO_2 produced in the resultant product gas. For this reason the following equations were used in order to calculate the carbon conversion (in 90 min at steady state) to gas:

$$C_a = C\ in\ CO + C\ in\ CH_4 \quad (1)$$

$$X_a = \frac{Ca}{initial\ carbon\ in\ char} \quad (2)$$

$$N = initial\ carbon\ in\ char - final\ carbon\ in\ char \qquad dW = \text{initial carbon in char - final carbon in char} \quad (3)$$

Eq. (1) calculates the carbon contained in the combustible (CO and CH_4) product gases and subsequently Eq. (2) calculates the carbon conversion (in 90 min at steady state) provided from via these gases from the char. Eq. (3) calculates the total quantity of char that has been converted into the product gases (in this case it is assumed into CO_2, CO and CH_4). In this study the carbon conversion and the cold gas efficiency are defined with Eqs. (4) and (5). Finally the lower heating value (MJ/N m^3) is the calorific value of the dry gas on a volumetric basis.

$$X = \frac{N}{Initial\ carbon\ in\ char} \qquad X = \frac{dW}{\text{Initial carbon in char}} \quad (4)$$

$$\mathrm{CGE}(\%) = \frac{Heating\ value\ of\ product\ gas}{Heating\ value\ of\ char} \quad (5)$$

Finally the oxygen supply rate and the H_2O/O_2 rate were calculated by mass balance from the reactions R3 and R4 in Table 2, by considering the flow rate of CO_2 and H_2O that were used in this study. The reason for that was because oxygen is the reactant gas which initiates gasification by raising the temperature in the cavity through R1 and R2. Oxygen is consumed fairly quickly and the CO_2 which is the main produced gas reacts with char according to R3. When stable gasification is achieved, H_2O is injected into the cavity to use the extra available heat and enhance the gasification performance with R4. Knowledge of oxygen and CO_2 supply rates and H_2O/O_2 and H_2O/CO_2 ratios are important for the UCG gasification performance since O_2 initiates the gasification and CO_2 drives it.

3 Results

3.1 Effect of temperature

Reaction temperature is a significant operating parameter which affects the gasification performance because the endothermic gasification reactions (R3 and R4) are favoured at high temperatures [4]. To study the effect of temperature the mass ratio of the H_2O/CO_2 was set to 2:1 according to previous commissioning experiments aimed at maximising the CO and H_2 concentration. The reactor pressure was fixed to 0.1 MPa (i.e. at atmospheric pressure). Fig. 5 shows how the concentrations of the produced gases evolved at (a) 750 °C and (b) 900 °C, in an atmosphere of CO_2 + H_2O (CO_2 flowrate of 0.4 l/min, H_2O/CO_2 ratio = 2:1) and a coal sample of 36 g.

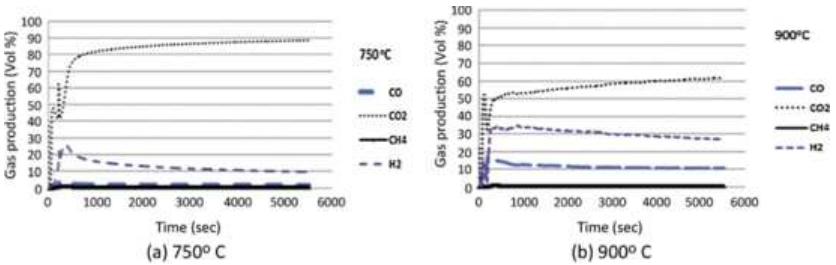

Fig. 5 Variation of concentration of the produced gases (vol%) over time at (a) 750 °C and (b) 900 °C under the flow of $CO_2 + H_2O$ ($H_2O/CO_2 = 2$, 0.1 MPa).

During the first 250 s of the reaction, the product gas concentrations are changing rapidly due to the steady state condition establishing in the reactor, which was characteristic of all the test conditions examined. It can be seen that when comparing the results at 750 °C and 900 °C, the concentration of the primary gaseous reactant (the CO_2) is notably lower in the 900 °C condition, yielding correspondingly higher concentrations of combustible product gases (notably CO and H_2).

It is subsequently apparent that an increase in temperature favours the carbon reduction reactions, enhancing the concentration of CO and H_2 and increasing the carbon conversion, LHV and CGE of the product gas as shown in Table 3. The CH_4 concentration remained unchanged implying that the hydrogasification reaction did not take place to any measurable extent, since CH_4 is produced mainly during the pyrolysis step.

Table 3 Gasification parameters of bituminous coal at different temperatures ($H_2O/CO_2 = 2$, 0.1 MPa).

T (°C)	600	750	800	850	900
Carbon conversion *X* (in 90 min at steady state)	0.006	0.02	0.06	0.10	0.24
LHV (MJ/N m^3)	0.4	1.7	1.9	3.0	4.9
CGE (%)	0.8	3.7	4.0	6.8	11.9

The effect of reaction temperature on the rates of char conversion to CO and CH_4 during CO_2–H_2O gasification of the bituminous coal is presented in Fig. 6a. It is clear that the gasification rate increases with increased reaction temperature for both reactions and the optimum temperature is 900 °C over the ranges tested; physical operating constraints from the rig meant that it was not possible to operate above this temperature. These results agree with other studies where the temperature effect on different coal chars under CO_2 and H_2O at atmospheric pressure was investigated and it was found that for the same reaction time (90 min at steady state) the carbon conversion increased with increasing temperature [12–14]. The maximum X_a was at 0.13.

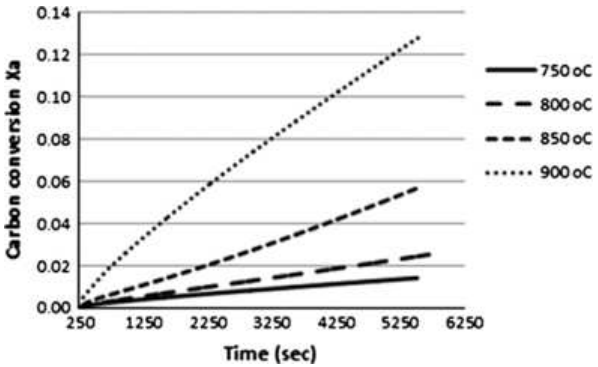

Fig. 6a Carbon conversion X_a of char to combustible gases (CO + CH_4) over time during $CO_2 + H_2O$ gasification at 750, 800, 850 and 900 °C ($H_2O/CO_2 = 2$, 0.1 MPa).

Previously published models were used to interpret the conversion-time data in Fig. 6a and it was found that the best correlation was via the shrinking core model of char with CO_2 and steam at 0.1 MPa. The reaction rate is expressed with the following equation [15]:

$$\frac{dX_a}{dt} = k(1 - X_a)^{2/3} \quad (6)$$

where *k* is the reaction constant and X_a is the carbon conversion of CO and CH_4. The integration of Eq. (6) results in a linear relationship between $(3(1 - (1 - X_a)^{1/3}))$ versus the reaction time as follows:

$$3(1 - (1 - X_a)^{1/3}) = kt \quad (7)$$

The reaction constant *k* can be derived from the slope of the straight line of Eq. (7) as calculated by Ahn et al. (2001) and shown in Fig. 6b [15]. The reaction constant *k* is described with the Arrhenius type Eq. (8) as follows:

$$k = Ae^{-(E/RT)} \quad (8)$$

where *A* is the pre-exponential factor, *E* is the apparent activation energy (kJ/mol) and *T* is the reaction temperature.

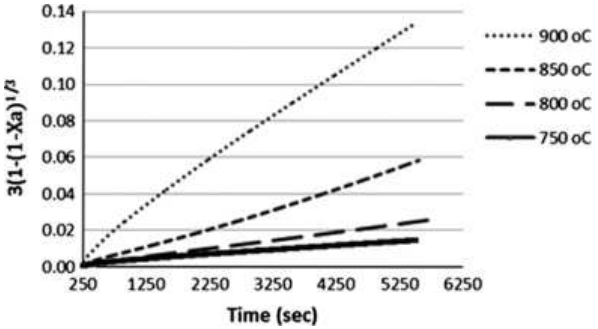

Fig. 6b Conversion data $3(1-(1-X_a)^{1/3})$ versus reaction time for $CO_2 + H_2O$ gasification at a total system pressure 0.1 MPa.

The Arrhenius plot for deriving the kinetic parameters of the reaction constant is illustrated in Fig. 6c. From the straight line fit of the reaction constant *k* at 0.1 MPa pressure and temperature range of 750~~to~~–900 °C, the activation energy *E* was derived to be 349.63 kJ/mol and the pre-exponential factor *A* was determined to be 5.~~83×104~~83×10^4/min. It is also evident that the gasification rate depends strongly on the temperature indicating chemical reaction rate control within the temperature range tested. These values are slightly higher than results published using TGA analysis for substantially smaller samples (100 mg) where char conversion was undertaken with single oxidising gases (such as CO_2 and H_2O) in individual reactions [16].

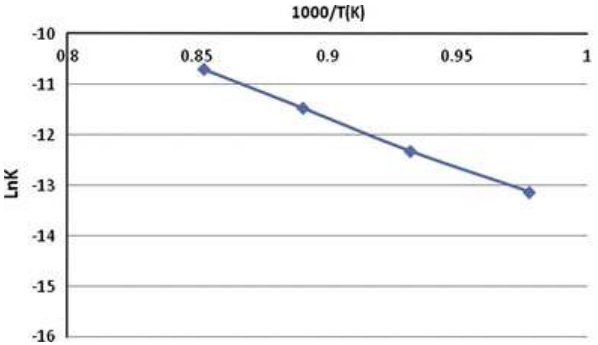

Fig. 6c Arrhenius plot of the reaction constant *k* for $CO_2 + H_2O$ gasification of the bituminous coal-char.

3.2 Effect of gasifying agent composition

The composition of the oxidants determines the composition of the gas produced and also the effectiveness of the gasification process. This parameter was studied by varying the mass of char in the reactor and the H_2O concentration. Fig. 7 shows the production of the gases during the gasification of the char using different H_2O/~~/~~CO_2 ratios at 900 °C and 0.1 MPa. It is shown that carbon steam gasification is enhanced as H_2O/~~/~~CO_2 ratio is increased but only up to (a) 3:1, above this ratio, at (b) 3.5:1 it is decreased because the concentrations of CO and H_2 are decreased and the concentration of CO_2 is increased.

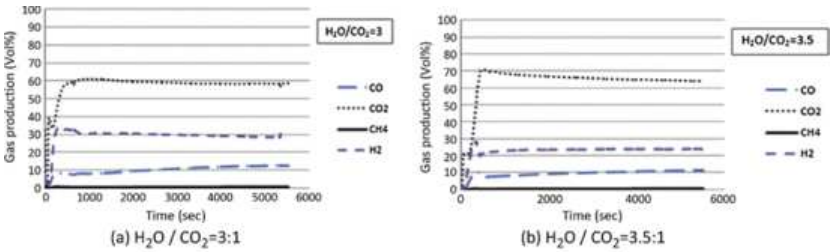

Fig. 7 Variation of concentration of produced gases (vol%) over time for (a) ratio of H_2O/CO_2 of 3:1 and (b) ratio of H_2O/CO_2 of 3.5:1 under the flow of $CO_2 + H_2O$ (900 °C, 0.1 MPa).

In Fig. 8 the carbon conversion (in 90 min at steady state) of the combustible gases (X_a) is plotted against time for various ratios of H_2O/CO_2 and it can be shown that the higher gasification rate was achieved with a ratio of 2:1 with the highest value of

X_a = 0.13, suggesting an optimum condition around this point. Above this ratio, the higher concentration of steam seems to decrease the gasification rate which can be explained by the adsorption–desorption mechanism proposed by different authors [17]. In this mechanism the retarding effect of the produced H_2 is taken into account which inhibits the char–steam reaction [18]. Furthermore in a two-step adsorption–desorption reaction mechanism, widely accepted for the char–CO_2 reaction at atmospheric pressure, the inhibiting effect of CO which slows down the gasification rate of the char–CO_2 reaction is taken into account [19,20].

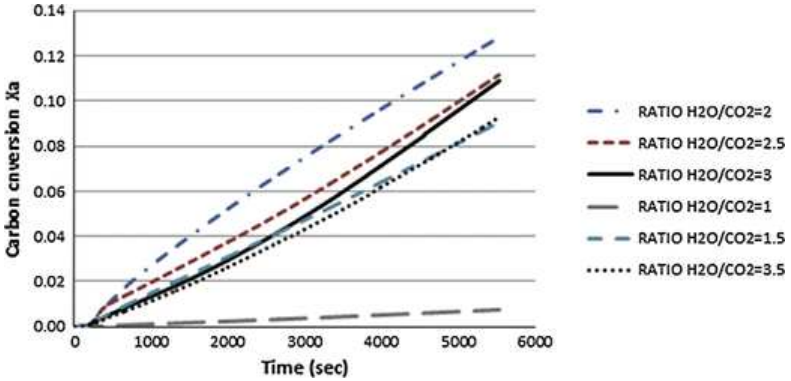

Fig. 8 Carbon conversion X_a of combustible gases (CO + CH_4) over time for various ratios of H_2O/CO_2 (900 °C, 0.1 MPa).

Figs. 9 and 10 show respectively the effect of the H_2O/CO_2 ratio on the gas production (mol/kg of sample) and the LHV (MJ/N m^3) of the product gas. In both cases the experiments were undertaken at 900 °C and 0.1 MPa (atmospheric pressure).

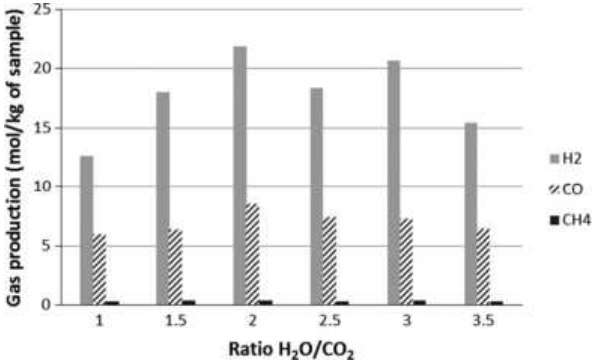

Fig. 9 Gas production (mol/kg of sample) during gasification of bituminous coal for various ratios of H_2O/CO_2 (900 °C, 0.1 MPa).

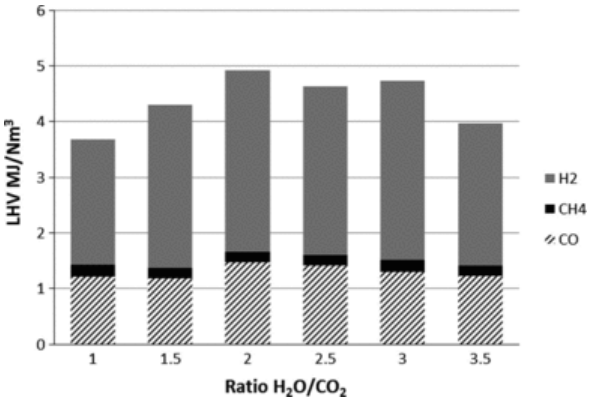

Fig. 10 LHV (MJ/N m^3) of the product gas during gasification of bituminous coal for various ratios of H_2O/CO_2 (900 °C, 0.1 MPa), expressed as the relative contributions of each gas.

Fig. 9 shows the production of the combustible product gases during the gasification of the coal with steam and CO_2 at different ratios. There is an increase in the H_2 concentration with an increase in the H_2O/CO_2 ratio, this decreases when the ratio of H_2O/CO_2 is above 3. The higher concentration of CO occurs between the H_2O/CO_2 ratios of 2–3 and the CH_4 concentration remains unchanged. This suggests that as the H_2O/CO_2 ratio increases, the gasification reactions R6 and R7 appear favoured to the detriment of reactions R3 and R4 but this phenomenon saturates above a H_2O/CO_2 ratio of 3:1.

As shown in Figs. 9 and 10, the H_2O/CO_2 ratio of 3:1 has a slightly higher concentration of H_2 than the ratio of 2.5:1, which gives a higher LHV at H_2O/CO_2 ratio of 3:1. This may be due to the small differences of the size of the coal samples, rather than a phenomenon relating to the reactant gas concentrations. Finally it can be noted that the range of the H_2O/CO_2 ratio between 2:1 and 3:1 provided optimum conditions, with LHV of 4.9 MJ/N m^3 (H_2O/CO_2 ratio of 2:1) as shown in Table 4.

Table 4 Gasification parameters of bituminous coal at different H_2O/CO_2 ratios (900 OC, 0.1 MPa).

H_2O/CO_2 ratio	1	1.5	2	2.5	3	3.5
Carbon conversion *X* (in 90 min at steady state)	0.12	0.16	0.24	0.23	0.21	0.12
LHV (MJ/N m^3)	3.7	4.3	4.9	4.6	4.7	3.9
CGE (%)	8.0	10	12.3	11.2	11.6	9.0

3.3 Effect of pressure

The effect of pressure on gas production during the gasification of the char was examined at a reactor temperature of 900 °C and a H_2O/CO_2 ratio of 2:1 and the results are presented in Fig. 11(a) at 0.9 MPa and Fig. 11(b) at 1.65 MPa. It can be observed that after approximately 500 s, which is the time required to reach steady state conditions in the reactor, the concentrations of CO, CH_4 and H_2 are comparatively higher and CO_2 was lower than that of the 0.1 MPa condition. The reason for this is that pressure increases the gas–solid contact, hence enhances the gas–solid reactions, favouring the CO, CH_4 and H_2 concentrations. Furthermore, at identical mass flow rates increasing the pressure increases the residence time so the gases have comparatively more time to react and reach equilibrium. This phenomenon saturates at higher pressures as it is shown in Fig. 11(c) at 2.2 MPa and Fig. 11(d) at 3.0 MPa where the resultant concentrations of CO_2 and CH_4 are subsequently higher and the concentrations of CO and H_2 are lower. At further higher pressures, the Le Chatelier–Brauns principal means that the equilibrium of reactions R5 and R7 will shift to the side with the fewer moles of gas, plus the inhibiting effect of CO and H_2 is considerably higher, so the concentration of CO_2 and CH_4 is favoured [4].

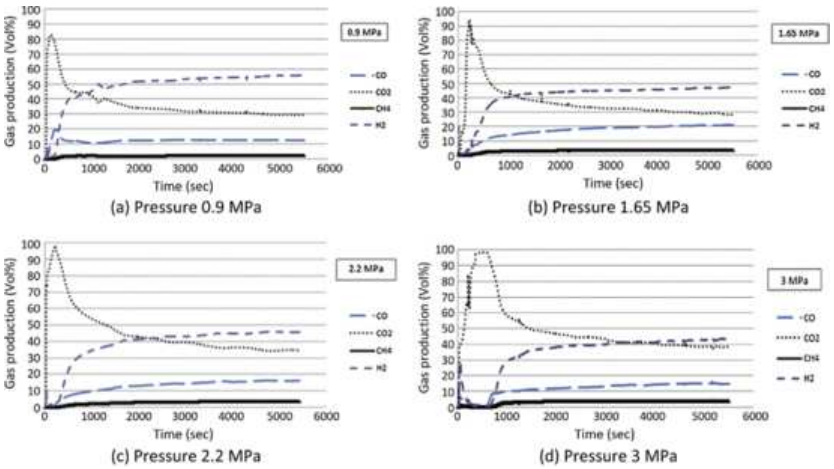

Fig. 11 Variation of concentration of product gas (vol%) over time for (a) 0.9, (b) 1.65, (c) 2.2 and (d) 3 MPa under a flow of CO_2 + H_2O (900 °C, H_2O/CO_2 = 2:1).

It can be noted that there was a significant reduction of the CO_2 concentration in the product gas under pressure compared to the ambient pressure condition in Fig. 5b. Under pressure the CO_2 concentration by volume was between 30% and 40% (Fig. 11) where in Fig. 5b the same experimental conditions were applied at atmospheric pressure, the CO_2 concentration by volume was between 50% and 60%.

Fig. 12 presents the gas production as a function of pressure which is shown in Table 5. It is noted that the maximum concentration of H_2 is produced for the pressures of 0.9 MPa and 1.65 MPa for the reasons explained above. It seems that there is a range of pressures which maximise the production of H_2.

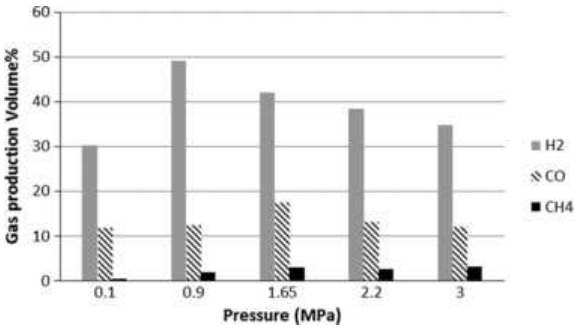

Fig. 12 Concentrations (vol%) of the combustible product gases over pressure.

Table 5 Average gas composition and LHV of product gas in CO_2 + H_2O gasification at 900 °C of the bituminous coal at a range of pressures.

Pressure	Gas composition			LHV	
	CO (vol%)	CH_4 (vol%)	H_2 (vol%)	MJ/N m^3	MJ/kg
0.1 MPa	11.8	0.5	30.2	4.9	3.9
0.9 MPa	12.3	1.9	49.1	7.5	7.2
1.65 MPa	17.4	2.9	42.1	7.8	7.5
2.2 MPa	12.9	2.8	38.9	6.8	6.1
3 MPa	11.9	3.1	34.7	6.4	5.7

In order to demonstrate the effect of pressure on the product gas compositions, the carbon conversion (as C in CO and CH_4) of the bituminous coal normalised to the total product gas flow rate during CO_2 + H_2O gasification at 900 °C and pressures from 0.1 to ~3 MPa is shown in Fig. 13. In this case the data has been normalised to take account of slightly different total mass flow rates through the reactor, which was caused by the effect of the pressure regulator located at the outlet of the rig. In undertaking this normalisation the data is expressed as the mass ratio of combustible gas species relative to the total product gas flow rate.

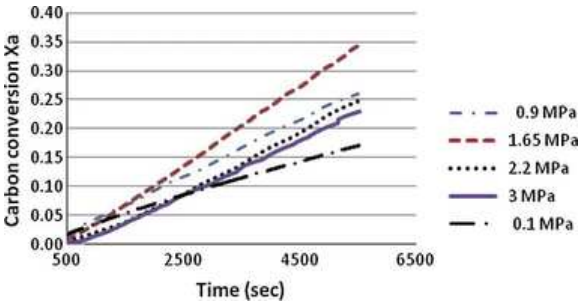

Fig. 13 Carbon conversion X_a of combustible gases (CO + CH_4) normalised over time during CO_2 + H_2O gasification at 900 °C and 0.1, 0.9, 1.65, 2.2 and 3 MPa.

Fig. 13 shows that the quantity of carbon converted (X_a) is notably increased by progressively higher pressures up to 1.65 MPa, above this pressure the incremental conversion becomes smaller which indicates that the effect saturates (over the conditions tested herein). From atmospheric pressure up to 1.65 MPa, this effect can be explained by the two-step reaction mechanism of adsorption – desorption which is shown as the following for the reactions R3 and R4 respectively [19,21–23].

$C + CO_2 \leftrightarrow C(O) + CO$	(R7)	Adsorption
$C(O) \rightarrow CO$	(R8)	Desorption
$C + H_2O \leftrightarrow C(O) + H_2$	(R9)	Adsorption
$C(O) \rightarrow CO$	(R10)	Desorption

C(O) are the adsorbed oxygen surface complexes and are determined by the forward adsorption reactions which influence the reaction rate. By increasing the pressure, the number of C(O) oxygen surface complexes formed will increase resulting in an increase in the reaction rate which is proportional to the number of these oxygen surface complexes [19,23,24]. At higher pressures as at 2.2 and 3.0 MPa, the formation of CO_2 and CH_4 has been observed from reactions R3 and R4 respectively, which can be explained by other mechanisms proposed by different authors [17,19,23,24]. With increasing the pressure further, the surface will be saturated with oxygen surface complexes which means that increases in pressure will not lead to the formation of further C(O) and the reaction rate will not increase so the impact of pressure becomes less significant to independent [19,25]. It appears that at pressures up to 1.65 MPa the controlling mechanism is adsorption because the oxygen surface complexes are increasing and at higher pressures, above 2.2 MPa the oxygen surface complexes approach saturation and the pressure effect becomes insignificant [16,19]. Furthermore during $C–CO_2$ and $C–H_2O$ gasification the reaction rate decreases as the pressure increases due to the increased inhibiting effect by CO and H_2 respectively [16,19].

Fig. 14 shows the carbon conversion of the bituminous coal at 900 °C under the flow of CO_2 and steam at different pressures. The data indicates that pressure has not had a significant impact on the carbon conversion with perhaps a slight increase between 0.9 and 1.65 MPa and a maximum value of $X = 0.28$ (of which combustibles gases, CO and CH_4, are $X_a = 0.13$). It appears that above 2 MPa the carbon conversion decreases but not significantly.

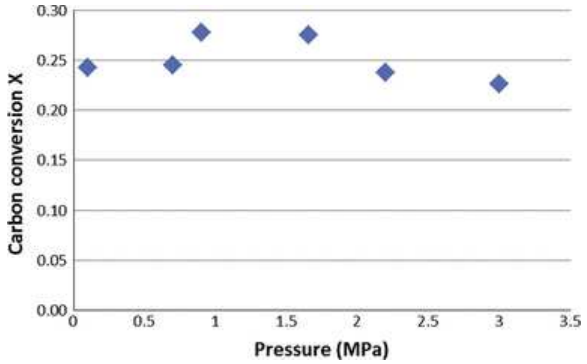

Fig. 14 Carbon conversion at 900 °C as a function of pressure.

The cold gas efficiency is presented as a function of pressure in Fig. 15, where it is shown that the CGE increases with pressure. The maximum cold gas efficiency was achieved for the range of pressures between 0.9 to 1.65 MPa and it seems that above around 2 MPa the CGE decreases. The maximum cold gas efficiency was measured at 26% over the range of conditions tested, which implies that around 26% of the available chemical energy of the char is converted to gas during this simulated reduction zone of a UCG cavity.

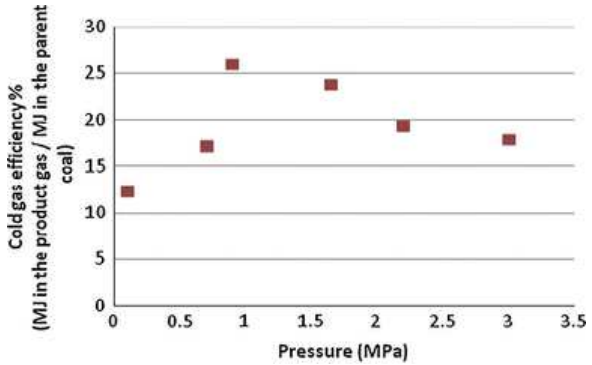

Fig. 15 Cold gas efficiency as function of pressure at 900 °C.

The LHV of the product gas is presented as a function of pressure in Fig. 16. The data shows that pressure increases the LHV of the product gas, with the highest value at 7.8 MJ/N m^3 at 1.65 MPa compared to the 4.9 MJ/N m^3 at 0.1 MPa. This provided a maximum gas yield of 0.6 kg of gas per kg of coal. Fig. 16 also indicates that the LHV of the product gas had its highest value between 0.9 to 1.65 MPa and it seems that above around 2 MPa the LHV decreases which is in good agreement with the carbon conversion and CGE result. Furthermore this finding agrees with a semi industrial test conducted with a coking coal (60% F.C, 16% V.M., LHV 26 MJ/kg) gasified with air and steam, aiming to investigate the effect of cyclically changing the operational pressure in terms of the quality of the product gas [26]. The gas composition was 15–25 % CO, 5–8% CH_4 and 10–30% H_2 which is in good agreement with the gas composition produced at pressures in this study for CO and H_2 during the reduction zone as shown in Table 5 and Fig. 12. The concentration of CH_4 is lower in the present study because CH_4 is mainly produced during the pyrolysis stage (Table 5), which was not considered in the research herein.

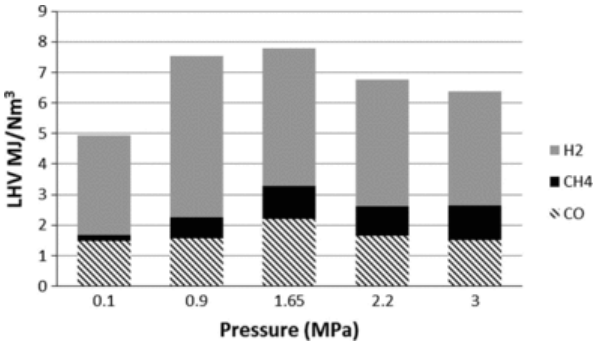

Fig. 16 LHV of the gas produced versus pressure during the reduction zone of a simulated UCG process expressed as energy contribution to the overall heating value of the resultant product gas.

3.4 Application of the data to UCG field trials

In this study it was found that the highest carbon conversion (in 90 min at steady state) was achieved at 0.28 during the reduction zone which means that 0.72 of the char was not gasified. Considering the data from the Rocky Mountain 1 field trial (where oxygen and steam were the oxidants) and the El Tremedial field trial (where oxygen and nitrogen were the oxidants) the carbon conversion was calculated as 0.54 (coal type 32% F.C, 32% V.M., HV = 20 MJ/kg) and 0.55 (coal type 36% F.C, 27.5% V.M., HV = 18 MJ/kg) respectively [10,27]. It must be borne in mind that these field trial values were achieved by including the volatile coal components and was reacted over 3 months for Rocky Mountain 1 and 12.1 days for El Tremedial. These field trials indicated that the carbon converted was approximately around 55% which means that 45% of char was left underground. This is in agreement with the sweep efficiency which is mentioned to be between 40% and 55% during a UCG process [8].

The maximum LHV of the product gas as measured in this laboratory investigation (Table 5) was found to be 7.5 MJ/kg at 1.65 MPa. Making an assumption that if the volatile fraction released during typical UCG operations were included, this coal would provide an LHV of around 10 MJ/kg [4] and hence the resultant CGE becomes around 40%. The bituminous coal tested had an LHV of 32 MJ/kg (V.M. = 13%, F.C = 83.2%), which is somewhat different to the coals used in the field trials under consideration. If the tested coal had the same LHV as that in the Rocky Mountain 1 field trial (HV = 20 MJ/kg) and the El Tremedial field trial (HV = 18 MJ/kg) then the resulting CGE would have been 60% and 66% respectively. Low rank coals with comparatively low heating values and high volatile matter content tend to have high CGE, but it should be borne in mind that the presence of volatile matter in UCG product gas is contributing significantly to the predicted CGE from the process, when compared with the conversion of fixed carbon to CO and CH_4.

In Fig. 17, the gas composition (mole %) of the Centralia field trial and Rocky Mountain 1 which were run at an operating pressure of 0.37–0.43 MPa and 0.5–0.7 MPa respectively with oxygen and steam used as oxidants, are plotted with the gas composition produced at the reduction zone of this study at 0.7 MPa. Furthermore in Fig. 18, the gas composition of El Tremedial (operating pressure of 5.4–5.6 MPa with oxygen and nitrogen as oxidants) is plotted with the gas composition of the product gas of this study produced at 3.0 MPa.

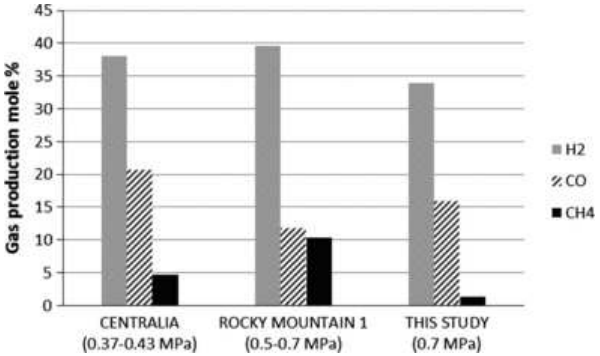

Fig. 17 Gas composition of Centralia field trial, Rocky Mountain 1 field trial and of this study at 0.7 MPa.

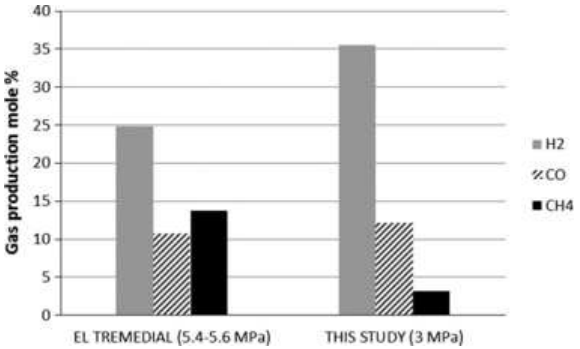

Fig. 18 Gas composition of El Tremedial field trial and of this study at 3.0 MPa.

It can be noted form both Figs. 17 and 18 that the concentrations of CO and H_2 of this study are comparable with those in the field trials, which reinforces the fact that the majority of the product gas, CO and H_2, is produced during the reduction zone. The concentration of CH_4 of this study is very low compared to the concentration of CH_4 of the field trials and that can be explained since CH_4 is mainly produced during the pyrolysis zone.

4 Conclusions

The analysis conducted in this paper has demonstrated the effects of a variety of parameters in the reduction reactions pertaining to the pressurised gasification of a bituminous coal. The optimum reduction conditions determined for the bituminous coal were H_2O/CO_2 = 2:1 (H_2O/O_2 = 2.4:1), 900 °C at 1.65 MPa. Under such conditions the product gas consists by volume of 17% CO, 3% CH_4 and 42% H_2 with a LHV of 7.8 MJ/N m^3. The maximum carbon conversion was 0.28 (in 90 min at steady state) of which 0.13 are CO and CH_4, the maximum CGE was 25.2% and the maximum gas yield was 0.6 kg of gas/kg of coal.

It should be noted that the results have allowed for the consistent analysis of the reduction processes, which yield combustible products directly from the solid phase char. This does not include the contribution of the volatile matter, hence this has in part demonstrated that typical UCG operations on low rank coals provides a combustible syngas product that relies heavily on releasing the volatile matter from the coal.

Pressure enhances the efficient energy conversion of coal to gas because it increases the heating value, carbon conversion, CGE and gasification rate of the bituminous coal and it seems that there was an optimum operating pressure which produces the maximum heating value of the product gas, over the conditions tested. Pressure maximises the H_2 production with a maximum measured concentration of 49% vol% at 0.9 MPa. Above the pressure of 2 MPa it appears that the effect of pressure saturates and only the CH_4 production is favoured with a maximum of 3 vol% at 3.0 MPa. There is a two step adsorption–desorption reaction mechanism that controls the process up to 1.65 MPa and the controlling step is adsorption. This was attributed to the oxygen surface complexes increasing with increasing pressure, which increases the gasification rate, but above 2.2 MPa the oxygen surface complexes reach saturation which means that the pressure effect does not enhance the reaction rate further.

Carbon conversion does not seem to be affected significantly by the type of coal and the amount of carbon converted to CO, CH_4 and CO_2 seems to be between 40% to and 55% but more investigation is needed to prove this definitively.

High rank coals can produce a good quality gas although the CGE will be apparently low due to their low volatile matter content. CGE is a parameter that determines gasification efficiency but the heating value of the produced gas is

equally important when considering the end use of the product gas.

The ratio of H_2O/CO_2 significantly affected the product gas composition above H_2O/CO_2 = 3:1. The H_2 production was maximised for the H_2O/CO_2 ratio of 2:1.

Temperature increases the gasification rate, carbon conversion, CGE and LHV of a UCG process significantly.

The shrinking core model predicted the reaction of char with CO_2 and steam at 0.1 MPa with reasonable accuracy. From the Arrhenius plot, the activation energy (E) was found to be around 350 kJ/mol and the pre-exponential factor (A) was determined to be 5.83×10483 × 10^4/min.

Acknowledgements

Financial support for the work in this paper has been received by the GRC's Seren project which is funded by the Welsh European Funding Office (WEFO). The financial support is gratefully acknowledged by the authors.

References

[1]

E. Shafirovich and A. Varma, Underground coal gasification: a brief review of current status, *Ind Eng Chem Res* **48** (17), 2009, 7865–7875.

[2]

A.W. Bhutto, A.A. Bazmi and G. Zahedi, Underground coal gasification: from fundamentals to applications, *Prog Energy Combust Sci* **39** (1), 2013, 189–214.

[3]

L. Yang, X. Zhang, S. Liu, L. Yu and W. Zhang, Field test of large-scale hydrogen manufacturing from underground coal gasification, *Int J Hydrogen Energy* **33** (4), 2008, 1275–1285.

[4]

R.H. Perry and D.W. Green, Perry's chemical engineers' handbook, 1999, M.Graw-Hill Companies Inc..

[5]

G. Liu and S. Niksa, Coal conversion submodels for design applications at elevated pressures. Part II. Char gasification, *Prog Energy Combust Sci* **30** (6), 2004, 679–717.

[6]

S. Porada, G. Czerski, T. Dziok, P. Grzywacz and D. Makowska, Kinetics of steam gasification of bituminous coal in terms of their use for underground coal gasification, *Fuel Process Technol* **130**, 2015, 282–291.

[7]

S. Krzysztof, et al., Experimental simulation of hard coal underground gasification for hydrogen production, *Fuel* **91** (1), 2012, 40–50.

[8]

D.W. Gregg and T.F. Edgar, Underground coal gasification, *AIChE J* **24** (5), 1978, 753–781.

[9]

D. Creedy, K. Garner, S. Holloway, N. Jones and T.X. Ren, Review of underground coal gasification advancements, 2001, DTI, Wardell Armstrong, BGS & Nottingham University, 64.

[10]

Chappell M, Mostade M. The El Tremedial underground coal gasification field test in Spain first trial at great depth and high pressure. in: Fifteenth annual international Pittsburgh coal conference 1998. Pittsburgh, USA; 1998.

[11]

S.-q. Liu, Y.-y. Wang and Y.N. Zhao, Enhanced-hydrogen gas production through underground gasification of lignite, *Min Sci Technol* **19** (3), 2009, 389–394.

[12]

J. Fermoso, et al., High-pressure co-gasification of coal with biomass and petroleum coke, *Fuel Process Technol* **90** (7–8), 2009, 926–932.

[13]

T. Liu, Y. Fang and Y. Wang, An experimental investigation into the gasification reactivity of chars prepared at high temperatures, *Fuel* **87** (4–5), 2008, 460–466.

[14]

D. Ye, J. Agnew and D. Zhang, Gasification of a South Australian low-rank coal with carbon dioxide and steam: kinetics and reactivity studies, *Fuel* **77** (11), 1998, 1209–1219.

[15]

D. Ahn, B.M. Gibbs, K.H. Ko and J.J. Kim, Gasification kinetics of an Indonesian sub-bituminous coal-char with CO_2 at elevated pressure, *Fuel* **80** (11), 2001, 1651–1658.

[16]

M. Irfan, M. Usman and K. Kusakabe, Coal gasification in CO_2 atmosphere and its kinetics since 1948: a brief review, *Energy* **36** (1), 2011, 12–40.

[17]

J.D. Blackwood and A.J. Ingeme, The reaction of carbon with carbon dioxide at high pressure, *Aust J Chem* **13** (2), 1960, 194–209.

[18]

F.J. Long and K.W. Sykes, The mechanism of steam carbon reaction, *Proc R Soc* **193**, 1948.

[19]

T. Wall, et al., The effects of pressure on coal reactions during pulverised coal combustion and gasification, *Prog Energy Combust Sci* **28** (5), 2002, 405–433.

[20]

D. Roberts and D. Harris, A kinetic analysis of coal char gasification reactions at high pressures, *Energy Fuels* **20** (6), 2006, 2314–2320.

[21]

P.L. Walker, F. Rusinko and L.G. Austin, Gas reactions of carbon, *Adv Catal* **11** (590), 1959, 133.

[22]

N.M. Laurendeau, Heterogeneous kinetics of coal char gasification and combustion, *Prog Energy Combust Sci* **4** (4), 1978, 221.

[23]

J.D. Blackwood and F. McGrory, The carbon steam reaction at high pressure, *Aust J Chem* **11** (1), 1958, 16–33.

[24]

H. Mühlen, K.H. van Heek and H. Jüntgen, Kinetic studies of steam gasification of char in the presence of H_2, CO_2 and CO, *Fuel* **64** (591), 1985.

[25]

D. Roberts and D. Harris, Char gasification with O_2, CO_2, and H_2O: effects of pressure on intrinsic reaction kinetics, *Energy Fuels* **14** (2), 2000, 483–489.

[26]

Q. Wang, Z.T. Wang and B. Feng, Semi industrial tests on enhanced underground coal gasification at Zhong-Liang-Shan coal mine, *Asia Pacific J Chem Eng* **4**, 2009, 771–779.

[27]

Britten J, Thorsness C. The Rocky Mountain 1 CRIP (Controlled Retracting Injection Point) experiment: Comparison of model predictions with field data. In: 14th annual underground coal gasification symposium 1988, Schaumburg, IL, USA; 1988.

Highlights

- Optimum gasification conditions were determined for the bituminous coal.
- Pressure enhances the gasification rate and hence the gasification efficiency.
- There is an optimum operation pressure which produces the best heating value of the product gas.
- Carbon conversion does not seem to be affected significantly by the type of coal.
- The shrinking core model predicts fairly well the reaction of char with CO_2 and steam at 0.1 MPa.

Queries and Answers

Query: Your article is registered as a regular item and is being processed for inclusion in a regular issue of the journal. If this is NOT correct and your article belongs to a Special Issue/Collection please contact aravind.kumar@elsevier.com immediately prior to returning your corrections.
Answer: IT IS CORRECT

Query: Please confirm that given name(s) and surname(s) have been identified correctly.
Answer: I CONFIRM THAT THE NAMES ARE CORRECT

Query: The usage of ‘Xa’ and ‘X_a’ seems to be inconsistent, hence it has been made consistent. Please check and amend if necessary.
Answer: I AM SATISFIED WITH Xa

Query: The unit ‘% vol has been changed to vol%. Please check and correct if necessary.
Answer: I am happy with vol%

Query: Please check the page range in all references and correct if necessary.
Answer: I am happy with the page range in the references

Query: Please check the year in Refs. [10,11,14,27].
Answer: The year in Reference [10] is correct The year in Reference [11] should change to 2008 The year in Reference [14] should change to 1997 The year in Reference [27] should change to 1989

Query: To maintain sequential order figures have been renumbered. Hence, their corresponding citations have also changed throughout the text. Please check, and correct if necessary.
Answer: It is correct